

# Performance of Geopier Reinforced Soil Foundations During Simulated Seismic Tests on I-15 Bridge Bents

Evert C. Lawton

Results are presented from full-scale tests on geopier foundations subjected to simulated seismic activity. The foundations were subjected to large cyclic lateral and uplift-compression loads as well as significant overturning moments produced by the horizontal forces. For the conditions of the tests, including large loads, poor subsurface soils, and no embedment of the foundations, the magnitudes of the maximum displacements and rotations were relatively small. Furthermore, the permanent displacements at the end of the tests were small. Overall the results indicate that geopier foundations are ductile and can sustain large displacements—such as those generated by earthquakes—without significant damage and can thereby maintain serviceability after an earthquake.

During May and June 1998, geotechnical testing was conducted in conjunction with structural testing on a section of the existing northbound I-15 bridge over South Temple in Salt Lake City, Utah. The tests were performed after the northbound bridge had been taken out of service, northbound traffic had been diverted to the existing southbound bridge, and the remainder of the northbound bridge had been demolished. The section of the bridge that was tested consisted of two bents and the deck and girders spanning the two bents (see Figure 1a). Cyclic lateral loads were applied to the bent caps to simulate seismic shaking during an earthquake.

A schematic elevation view of the testing setup is shown in Figure 1b. The anticipated maximum lateral load to be induced on the bent caps was 1.78 MN (400 kips). During the actual testing a maximum lateral load of 2.18 MN (490 kips) was induced. The cyclic lateral loads were applied to the bent caps using a hydraulic actuator attached to a steel reaction frame, which was founded on two reinforced concrete footings newly constructed for this research project. Each footing was 7.48 m (24.5 ft) long, 2.51 m (8.25 ft) wide, and 1.0 m (3.25 ft) thick and was supported by 10 uplift geopiers (see Figure 2).

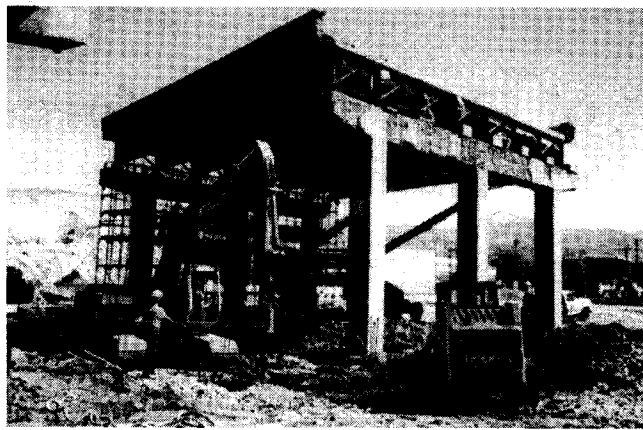
The forces generated by cyclic pushing and pulling on a bent cap are illustrated in Figure 1b for the anticipated maximum lateral force of 1.78 MN (400 kips). This pushing force produced a compressive force of 2.22 MN (500 kips) on the exterior footing and an uplift force of the same magnitude on the interior footing. During pulling, the same magnitude of vertical forces was produced, with uplift on the exterior footing and compression on the interior footing. The two reaction frame footings were founded on

the ground surface, so the resistance to the lateral loads was produced by shearing along the footing-soil interface as well as by pushing of the threaded uplift bars into the geopiers. This horizontal force couple produced an overturning moment on each footing, with a moment arm somewhat greater than the thickness of the footing.

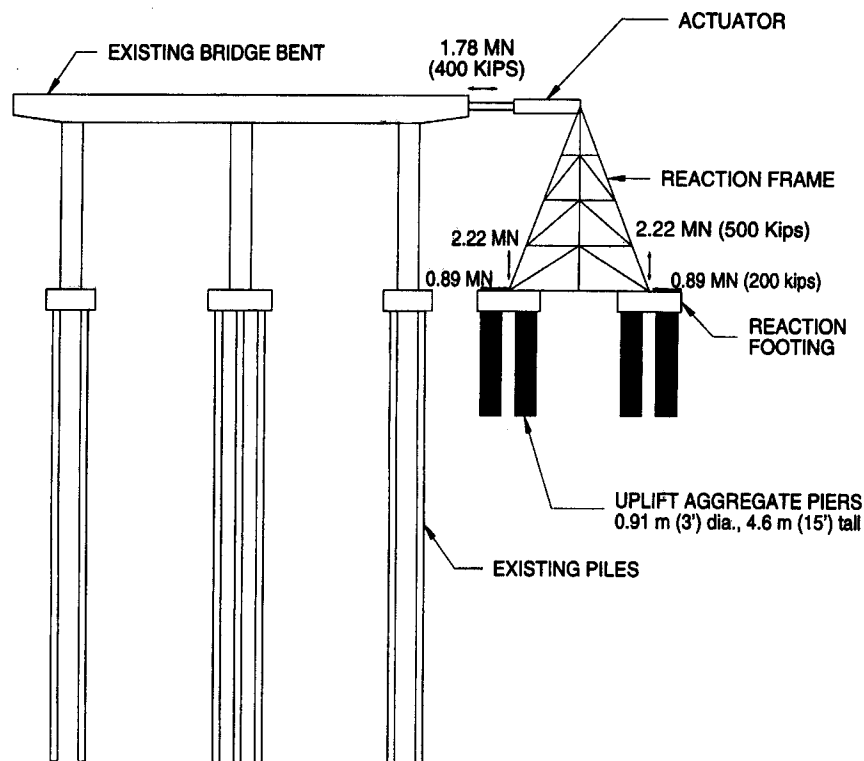
A series of three structural tests was performed on the two bents. The first structural test was conducted on May 23, 1998, on the southern bent (Bent 5) in the "as-is" condition. The second structural test was performed on June 6, 1998, on the northern bent (Bent 6), which had been previously wrapped with carbon fiber composites around the joints where the three columns intersect the cap. The purpose of this test was to determine the effectiveness of carbon fiber composites in providing additional strength and ductility if installed before an earthquake. The third structural test was conducted on June 27, 1998, on Bent 5 after it had been wrapped with carbon fiber composites after being tested to failure on May 23. The purpose of this test was to determine if carbon fiber composites can be used to restore a bridge to service after the bents have failed during an earthquake.

Analysis of the pile caps supporting these two bents indicated that the piles might fail laterally during the tests. To prevent this from occurring during the three structural tests described above, the pile caps were tied structurally to the reaction frame footings to limit the amount of lateral movement. Following the second and third structural tests, the lateral bracing systems were disconnected so that the pile caps and the reaction frame footings would move without artificial restraint. Geotechnical tests were then conducted in which the bent was pushed in a cyclic manner similar to that used for the structural tests.

A geopier foundation system is one of the few soil improvement methods that can safely carry significant lateral and uplift forces. Details on the method of installation of geopiers and their behavior under compressive and uplift loads can be found elsewhere (1, 2). The method of installation consists of opening holes in the ground by augering or excavation and filling the cavities with highly densified granular material by means of a specially designed tamper using high-energy, low-frequency impact procedures. Where large lateral and uplift capacities are needed, a steel plate is inserted at the bottom of each hole, with vertical steel uplift bars attached to the plate near its perimeter. The bars are extended past the tops of the geopiers into a footing and become bonded to the footing when the concrete is placed. Uplift and passive resistance are mobilized in a geopier when the footing moves, pulling on the bars. Additional lateral resistance is also generated by the high



(a)



(b)

**FIGURE 1** Pushover tests on bridge bents: (a) looking northeastward at the two bents tested; (b) schematic representation of test setup.

shearing resistance along the footing-geopier interfaces at the bearing level.

The primary purpose of the geotechnical tests was to verify under full-scale conditions the mechanisms by which geopier foundations resist lateral, compressive, and uplift loads. Furthermore, it was desired to determine if geopier foundations can be used successfully to support structures in regions of high seismic potential. The technical discussion in this paper relates to the performance of the

geopier foundations supporting the structural reaction frames during the geotechnical tests.

#### SITE GEOLOGY AND SUBSOIL CONDITIONS

Results from a typical cone penetration test (CPT) conducted at the site are shown in Figure 3. The upper 6 m (20 ft) is recent (Holocene)

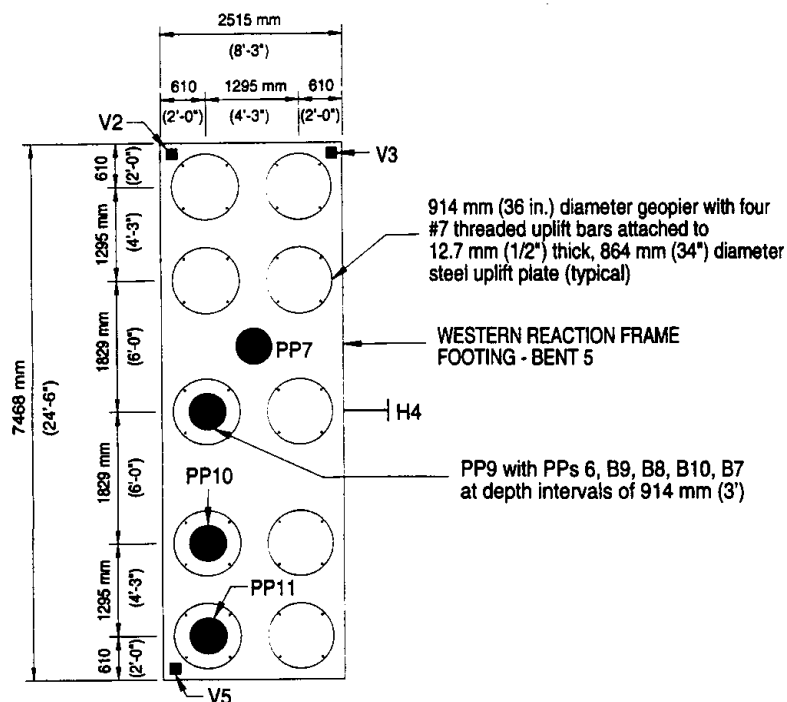


FIGURE 2 Footing dimensions and locations of geopiers and primary instrumentation (PP = pressure plate).

alluvium from streams and creeks coming out of the major canyons. These soils are primarily low-plasticity silty clays and clayey silts (CL, ML), although there are some zones of highly plastic clays. Interbedded within these cohesive materials are generally thin layers of sand, which are indicated in Figure 3 by high values of  $q_c$  and  $f_R < 1$  percent. Bonneville clay is present at depths of about 6 to 17 m (20 to 56 ft) and is Pleistocene in age. These clays are generally soft and highly compressible. There are some fine sand interbeds within the Bonneville clay, which are predominant in the middle of the layer.

### FULL-SCALE GEOTECHNICAL TESTS

Procedures and results of both geotechnical tests are similar, so the discussion here will be restricted to the second geotechnical test. The loads were applied to the bridge bent by alternately pushing and pulling on the cap in cycles of gradually increasing horizontal displacement. In the second test, the cap was first pushed and then pulled laterally a maximum distance of 25 mm (1 in.) and then this same displacement pattern was repeated. This procedure was repeated for maximum displacements of 50 to 203 mm (2 to 8 in.)

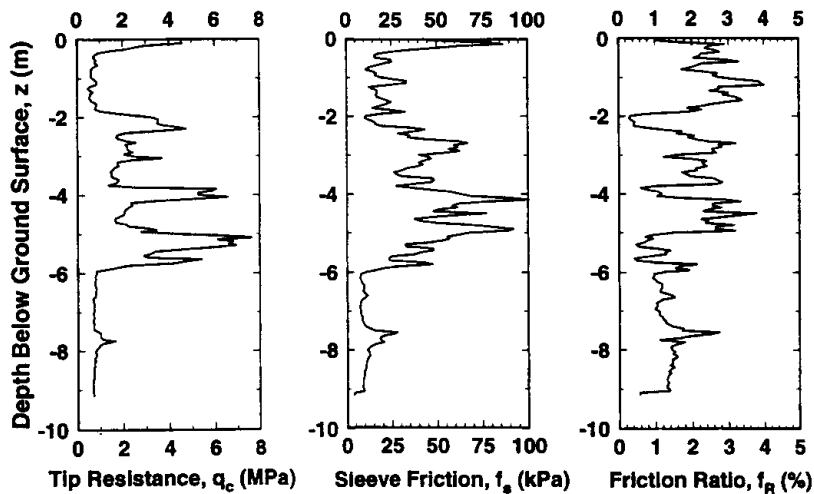


FIGURE 3 Typical CPT profile for site.

in increments of 25 mm (1 in.). The cap was then pushed a maximum distance of 229 mm (9 in.) and then pulled back to zero displacement, and this pattern was repeated for a second cycle. This procedure was then used for maximum displacements of 254, 279, and 305 mm (10, 11, and 12 in.). This modified procedure at maximum displacements of 229 mm (9 in.) and higher was necessitated by limitations on the stroke of the actuator and stretching of the prestressing strands used to pull back on the cap. The horizontal displacements of the cap as a function of elapsed time are shown in Figure 4a. These displacements of the bent cap were measured from its original location before the start of the test.

Shown in Figure 4b is the measured lateral force on the bent cap versus elapsed time. It can be seen that the magnitudes of the lateral forces at the same level of displacement for the pushing and pulling portions of the same cycle were not the same. For example, during the second push-pull cycle at a maximum displacement of 203 mm (8 in.), the force at the maximum displacement during the push cycle was 1045 kN (235 kips), whereas the force at the same maximum displacement during the pull cycle was 1579 kN (355 kips). These disparities are likely related to permanent damage done to the superstructure of the bent during the structural test and also during the geotechnical test as well as net movements of the pile caps during testing.

## Induced Vertical Compressive Stresses

### Footing Contact Stresses During Compressive Loading

A geopier foundation is a composite system consisting of stiff, strong cylindrical inclusions within a matrix of weaker, more compressible native soil. A rigid footing carrying a centric vertical load will settle uniformly on any stable bearing system. For a rigid footing settling uniformly on a geopier foundation system, stress-deformation compatibility dictates that the induced contact stresses on the stiffer geopiers be greater than the stresses induced on the more compressible matrix soil. Using subgrade reaction theory (3), Lawton et al.

(2) showed that the following equations apply for the contact stresses induced by a rigid footing on the supporting geopiers and matrix soil:

$$\Delta q_g = \Delta q \cdot \frac{R_s}{R_s(R_s - 1) + 1} \quad (1)$$

$$\Delta q_m = \Delta q \cdot \frac{1}{R_s(R_s - 1) + 1} = \frac{\Delta q_p}{R_s} \quad (2)$$

where

$\Delta q_g$  = induced contact stress on geopiers,

$\Delta q_m$  = induced contact stress on matrix soil,

$\Delta q$  = average induced contact stress,

$R_s$  = area replacement ratio =  $A_g/A$ ,

$R_s$  = subgrade modulus ratio =  $k_g/k_m$ ,

$k_g$  = subgrade modulus of geopiers =  $\Delta q_g/S$ .

$k_m$  = subgrade modulus of matrix soil =  $\Delta q_m/S$ , and

$S$  = average settlement of rigid footing.

To measure induced contact stresses, three pressure plates (PP) were placed on top of selected geopiers and one pressure plate was placed on top of the matrix soil at the locations shown in Figure 2. The concrete for the footings was poured directly on top of the pressure plates. Measured stresses for the four pressure plates are shown in Figure 5 for the first push cycle at a maximum displacement of 203 mm (8 in.). It is apparent that the stresses induced on the geopiers were substantially greater than those induced on the matrix soil. At the peak of the push cycle, which occurred at an elapsed time of 73.3 min, the measured induced stresses in the pressure plates on top of the geopiers were 244, 182, and 207 kPa (35.4, 26.4, and 30.0 psi) for PP 9, 10, and 11, respectively. The corresponding induced stress on top of the matrix soil as measured by PP 7 was 5.3 kPa (0.77 psi).

One method of assessing the reasonableness of these measured stresses was to estimate the total applied vertical force at the peak of the push cycle by assuming the load to be centric and multiplying the measured stresses by the appropriate contact areas. This assumption results in assumed stresses of 244 kPa (35.4 psi) on the

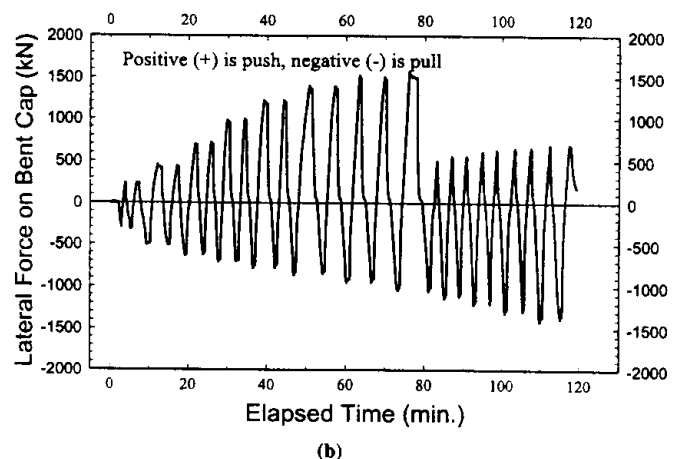
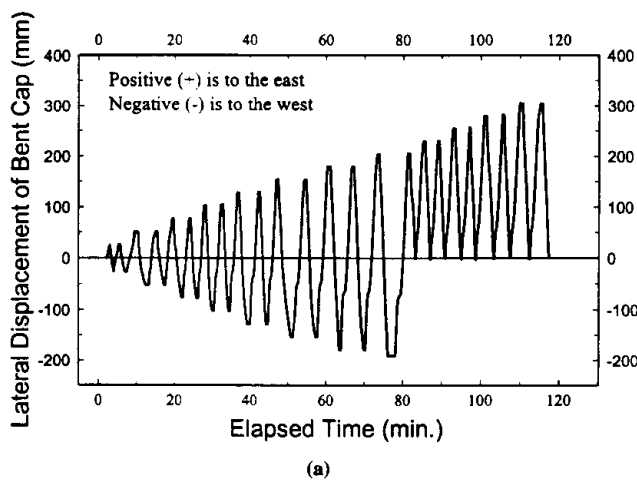


FIGURE 4 Results from lateral pushing during second geotechnical test on June 27, 1998: (a) lateral displacement of bent cap; (b) lateral force on bent cap.

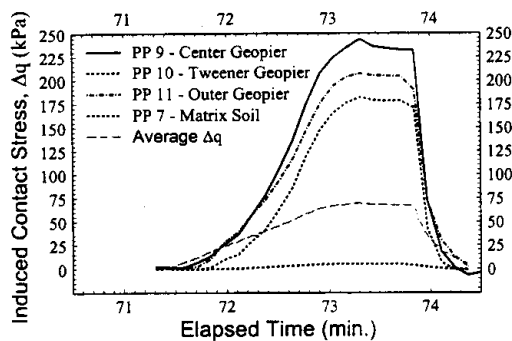


FIGURE 5 Measured induced footing contact stresses on geopiers and matrix soil.

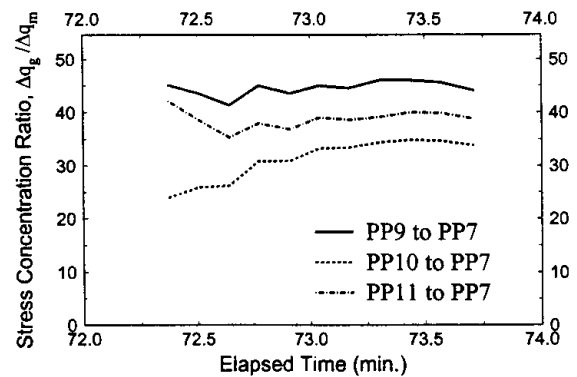
two center geopiers, 182 kPa (26.4 psi) on the four intermediate geopiers, and 207 kPa (30.0 psi) on the four corner geopiers. Using the nominal diameter of the geopiers to calculate the contact areas for the geopiers gives an estimated total force of 1343 kN (302 kips) carried by the geopiers. Similarly, assuming the stress on the matrix soil to be 5.3 kPa (0.77 psi) at all locations and multiplying this stress by the area of matrix soil gives an estimated total force of 67 kN (15 kips) carried by the matrix soil. Thus, the total estimated force induced on the footing by the pushing is 1410 kN (317 kips) using this method.

A second estimate was obtained by multiplying the measured lateral force applied to the bent cap 1045 kN (235.0 kips) by the appropriate multiplication factor of 1.25 obtained from static analysis of the reaction frame assuming the supports to be hinged. This method gives an estimated vertical force of 1307 kN (294 kips). Comparing the two predicted values shows that Method 1 gives a value 8 percent greater than that using Method 2. Therefore, it appears that the measured values of induced stress are reasonable.

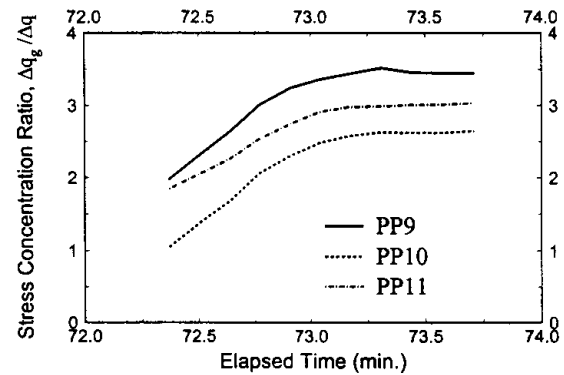
A number of actual conditions vary from those assumed above. As will be shown in a subsequent section, the applied loads were eccentric. There was significant rotation of the top of the western footing from east to west, which would result in lower stresses on the geopiers on the east side of the footing compared with those on the west side. In addition, there was some small rotation from south to north, which would have generated slightly higher stresses on the geopiers on the northern side of the footing than on those on the southern side. The actual diameters of the geopiers were somewhat larger than the nominal diameter owing to pushing of the geopier material laterally into the adjacent matrix soil during installation. These factors offset each other to some extent with respect to the estimated vertical load, so the measured values of stress still appear to be reasonable.

The measured induced stresses yield stress concentration ratios ( $\Delta q_g/\Delta q_m$ ) of 46, 34, and 39 for PP 9, 10, and 11 compared with PP 7. The stress concentration ratios versus time are shown in Figure 6a for the main part of the push cycle and range from approximately 25 to 45. The values at the beginning and end of the cycle are not shown because they were erratic owing to inaccuracies in measuring  $\Delta q_m$  at very low stress levels.

Also shown in Figure 6a is average induced contact stress ( $\Delta q$ ) versus time, calculated as the induced vertical stress divided by the area of the footing. To determine if Equations 1 and 2 can be used to provide reasonable estimates of  $\Delta q_g$  and  $\Delta q_m$ , calculations were performed using the data shown in Figure 5. The area replacement



(a)



(b)

FIGURE 6 Stress concentration ratios: (a)  $\Delta q_g/\Delta q_m$ ; (b)  $\Delta q_g/\Delta q$ .

ratio is calculated as the area of the 10 geopiers divided by the area of the footing, which gives  $R_a = 0.350$ . If it is assumed that the settlement of the footing at the location of all four pressure plates was about the same, which is reasonably correct, the stress concentration ratios are approximately equal to the subgrade modulus ratio,  $R_s$ . Thus, a reasonable range for  $R_s$  is 25 to 45. From Equation 1 it is found that the calculated values of  $\Delta q_g/\Delta q$  are not sensitive to  $R_s$ , with  $\Delta q_g/\Delta q$  varying from 2.65 for  $R_s = 25$  to 2.74 for  $R_s = 45$ . Values of  $\Delta q_g/\Delta q$  determined from the test data are plotted versus time in Figure 6b for the same time range as in Figure 6a. Although the values of  $\Delta q_g/\Delta q$  shown in Figure 6b vary from 1.0 to 3.5, the variation is much less (2.6 to 3.5) over the time period of 73.0 to 73.7 min, which is also the period for which the values of  $\Delta q_g/\Delta q_m$  are nearly constant for each pressure plate. The average value of  $\Delta q_g/\Delta q = 2.7$  calculated from Equation 1 is within the range of measured values (2.6 to 3.5) for the time period for which the data seem most consistent. Therefore, it appears that Equation 1 can be used to provide a reasonable estimate of  $\Delta q_g$  if  $R_s$  is known or can be reliably estimated.

Estimates of  $\Delta q_m/\Delta q$  using Equation 2 are fairly sensitive to the value of  $R_s$ , varying from 0.11 to 0.06 for  $R_s = 25$  to 45. Values determined from measured data range from 0.04 to 0.08, with values between 0.07 and 0.08 for the time period 73.0 to 73.7 min. Therefore, it appears that Equation 2 can be used to give reasonable estimates of  $\Delta q_m$ . Since the matrix soil carries so little stress compared

with that carried by the geopiers, the estimate of settlement for a geopier foundation system generally does not depend significantly on the estimated magnitude of  $\Delta q_m$ .

*Distribution of Induced Vertical Stress Within Geopiers*

Within the central geopier of the western footing that had PP 9 on top, five additional plates were placed at depth intervals of 0.91 m (3 ft) within the geopier (see Figure 2). These pressure plates, along with PP 9, were located so as to provide information on the distribution of vertical stress within that geopier. Unfortunately, PPB7, which was placed on the top of the uplift plate, was damaged during installation of the geopier.

The measured induced compressive vertical stress for these pressure plates is plotted in Figure 7a for the first push-pull cycle at a maximum displacement of the bent cap of 203 mm (8 in.). During the push cycle, which applied a compressive vertical force to this footing,  $\Delta\sigma_v$  was greatest at the top of the geopier and decreased

with increasing depth within the geopier. During the pull cycle, uplift forces were induced on the footing and the loads were transferred to the geopiers by the uplift plates at the bottoms of the geopiers. Thus, the plates located near the bottom of the geopier had the largest induced compressive stresses, and the induced stresses decreased with increasing distance above the bottom of the geopier.

The results for the first push cycle at maximum displacements of the bent caps of 203, 254, 305 mm (8, 10, and 12 in.) are shown in normalized fashion in Figure 7b for the first push cycle. The normalized results are nearly the same for all three push cycles and show that the induced compressive stresses dissipate quickly with depth within the geopier. For example, the induced stress reaches a level of 10 percent of the stress at the top of the geopier at a depth of about 3.0 m (10 ft). This depth is 3.3 times the diameter of the geopier and 1.2 times the width of the footing. Preliminary simplified theoretical analyses indicate that the induced stresses in the geopier at the greatest depth measured ( $z/d_g = 4$ ) are less than what would occur for the same footing carrying the same load bearing on a homogeneous soil.

**Displacements of Reaction Frame Footings**

*Horizontal Displacements*

The structural reaction frame rigidly tied the two footings together so that they moved laterally as a unit. This movement was proved during the testing by placing a displacement transducer between the two footings to monitor differential lateral movement. The footings were founded on the ground surface and thus were not embedded. Therefore, the only two mechanisms available for resisting lateral loads were shearing resistance along the bottom of the footing and passive resistance from the threaded uplift bars being pushed into the geopiers.

The lateral displacements of the footing versus elapsed time during the test are shown in Figure 8a. Inspection of the peak displacements for each set of load cycles at the same displacement level of the bent cap shows some interesting results. During each set of two push cycles, there was little net displacement after the second push compared with the first push except for the last two cycles, in which a small net displacement to the west occurred. In contrast, during the pull cycles, some noticeable net displacement to the east occurred on the second push compared with the first push for every cycle except the first two. As shown in Figure 4b, the peak forces for each set of two push or pull cycles was essentially the same. The reason for this difference in force-displacement behavior between the push and pull cycles is not known. At the final time when the force was zero (elapsed time of 116.3 min.), there was a net displacement of about 23 mm (0.9 in.) to the east.

The relationships of lateral force versus lateral displacement for the entire test are shown in Figure 8b. A maximum displacement of 46 mm (1.8 in.) occurred during the push cycles at a force of 1357 kN (305 kips). For the pull cycles, a maximum displacement of 41 mm (1.6 in.) occurred at a force of 1579 kN (355 kips). Considering that the total dead load acting on both footings was only about 890 kN (200 kips) and that the footings were not embedded, these maximum displacements are small. At high displacements or lateral loads, the stiffness of the geopier foundation system increases significantly with increasing displacement or force. Furthermore, these results show that geopier foundations are ductile and can sustain large

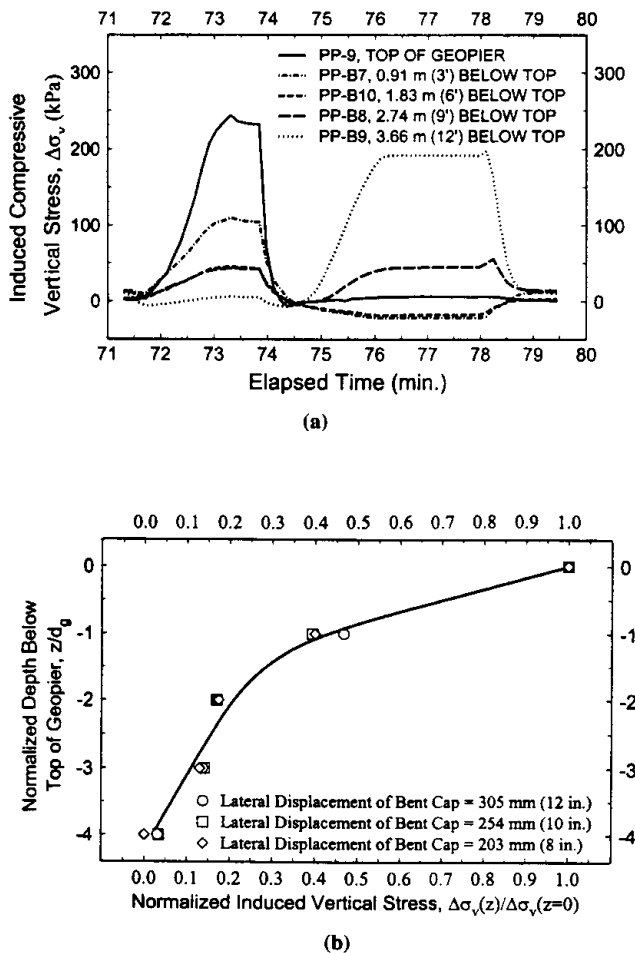
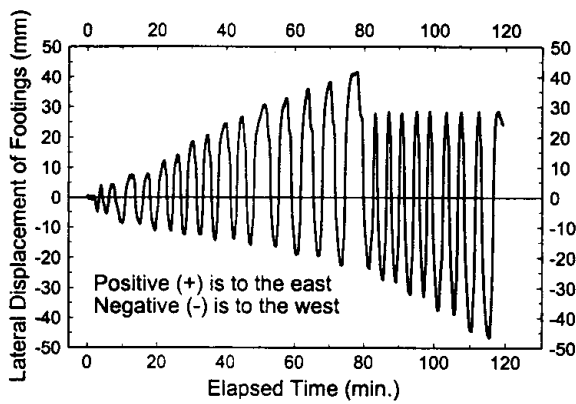
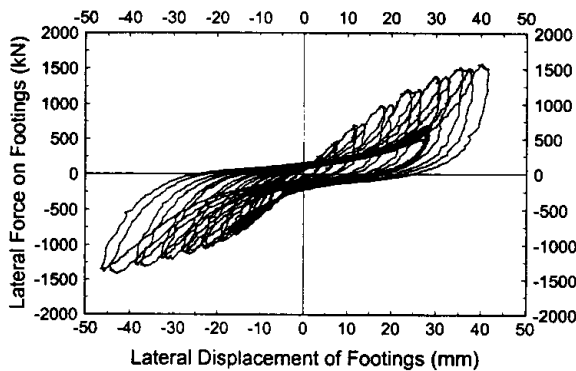


FIGURE 7 Induced compressive stresses within geopier: (a) at various depths within central geopier of western reaction frame footing; (b) normalized induced compressive stress as function of normalized depth.



(a)



(b)

FIGURE 8 Lateral displacements of footings: (a) versus elapsed time; (b) versus lateral force.

deformations—such as those generated by earthquakes—without significant damage or large permanent displacements.

Footings bearings on geopier foundation systems have high lateral sliding capacities owing to the effect of vertical stress concentration. A high percentage of the total vertical load is carried by the geopiers, which are much stronger than the matrix soil. Owing to length limitations, only a brief discussion of the maximum lateral capacity of the geopier foundations in these tests will be provided. Additional details may be found elsewhere (4).

The general equation for the maximum lateral resistance provided by shearing along the bottom of a footing bearing on a geopier foundation system ( $R_{hs}$ ) is as follows:

$$R_{hs} = V_g \tan \phi_g + V_m \tan \phi_r + A_m c_m \quad (3)$$

where

$V_g$  = total compressive vertical force acting on geopiers =  $q_g A_g$ ,

$V_m$  = total vertical force acting on matrix soil =  $q_m A_m$ ,

$A_g$  = area of geopiers beneath footing, and

$A_m$  = area of matrix soil beneath footing.

Friction angle  $\phi_g$  was estimated to be 50 degrees from results of a CPT pushed through a geopier. Measured values of friction angles for geopiers from full-scale direct shear tests on geopiers have

ranged from 48 to 53 degrees, so this estimated value is reasonable. Preliminary tests indicate that the silty clay at the bearing level of the footings was overconsolidated, with a preconsolidation pressure of about 34 kPa (720 psf). In the overconsolidated range, the peak strength parameters were  $\phi \approx 26$  degrees and  $c \approx 10$  kPa (210 psf). In the normally consolidated range, peak values were  $\phi \approx 38$  degrees and  $c \approx 0$ . Using Equation 3 and the appropriate strength parameters, the estimated value of  $R_{hs}$  was 2930 kN (658 kips). A numerical analysis of the passive lateral resistance provided by the uplift bars was conducted using the lateral pile program COM624 (5). At a displacement of 0.06 mm (1.6 in.) corresponding to the maximum lateral force of 1579 kN (355 kips), the estimate lateral resistance from the uplift bars was 658 kN (148 kips). The combined maximum lateral resistance of 3588 kN (806 kips) yields a factor of safety against lateral failure of 2.3. The estimated maximum lateral capacity of the same size footing without geopiers was 485 kN (109 kips).

### Vertical Displacements

Three transducers were used to measure the vertical displacement of each reaction frame footing (see Figure 2). The vertical displacements of the western footing for the entire test are shown in Figure 9 for the entire test. The peak upward displacement of 21 mm (0.82 in.) occurred in the northwest corner of the footing at an elapsed time of 76.1 min under an uplift force of 1975 kN (444 kips). The other measured displacements of the footing at that time were 14 mm (0.56 in.) in the southwest corner and 8.0 mm (0.32 in.) in the northeast corner. The maximum downward displacement of -11 mm (-0.42 in.) occurred in the northwest corner at an elapsed time of 110.0 min. The corresponding displacements at the other locations were -10 mm (-0.41 in.) in the southwest corner and -2.0 mm (-0.08 in.) in the northeast corner. The vertical displacements of the footing the last time the force was zero (elapsed time of 116.3 min.) were -1.8 mm (-0.07 in.) for the northwest corner, -0.51 mm (-0.02 in.) for the northeast corner, and -3.0 mm (-0.12 in.) for the southwest corner.

The results for the first push-pull cycle at a maximum bent cap displacement of 203 mm (8 in.) are shown in Figure 10a. The net displacements are calculated as the displacements from the original position of the footing at the start of this cycle. When the results for the displacements in the northwest corner are compared with

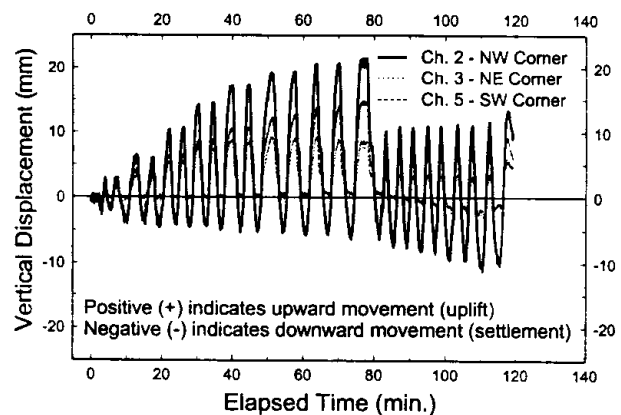


FIGURE 9 Vertical displacements of the western reaction frame footing for entire test.

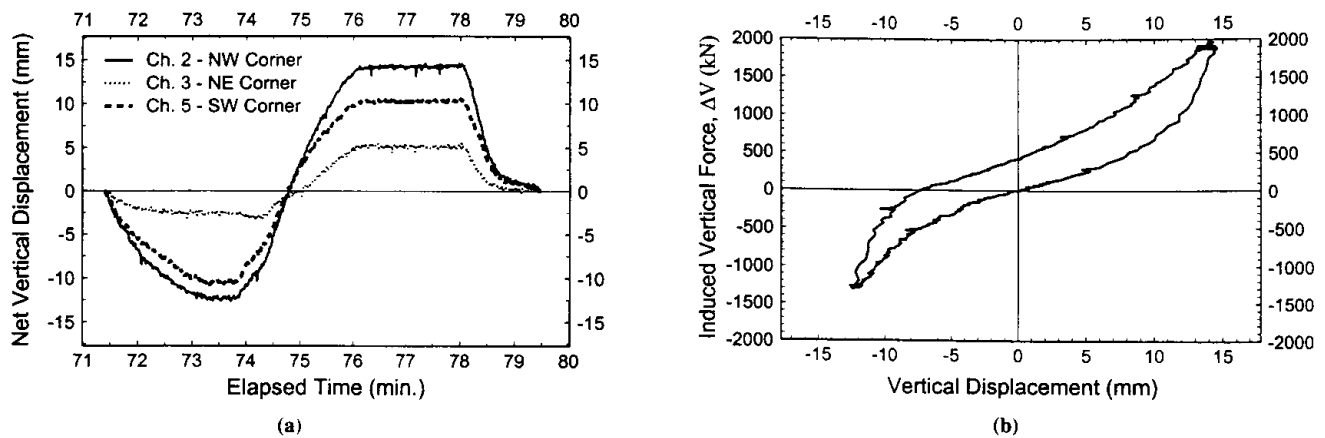


FIGURE 10 Net vertical displacements of western reaction frame footing for first push-pull cycle at a maximum bent cap displacement of 203 mm (8 in.): (a) versus elapsed time; (b) versus induced vertical force.

those in the northeast corner, it can be seen that rotation occurred in the direction of the overturning moment for both the push and pull cycles. During the push cycle, the lateral force on the footings was to the west and the vertical force was compressive. The primary lateral resistance developed as shear along the footing base to the east, producing an overturning moment that rotated the top of the footing from east to west. During the pull cycle, the lateral force on the footings was to the east and the vertical force was uplift. The primary lateral resistance developed as shear along the footing base to the west, producing an overturning moment that rotated the top of the footing from west to east. It can also be seen that there was some small transverse rotation during the push cycle, with greater rotation during the pull cycle. This finding occurred throughout the test and indicates that the direction of the pulling force was farther out of alignment with the bent cap than the pushing force. The maximum settlement of the footing for this cycle was  $-12$  mm ( $-0.49$  in.) in the northwest corner under a compressive vertical force of 1308 kN (294 kips) and an overturning moment of at least 1296 kN-m (956 ft-kips). The maximum uplift was 15 mm (0.58 in.), also in the northwest corner, under an uplift vertical force of 1975 kN (444 kips) and an overturning moment of at least 1953 kN-m (1,440 ft-kips).

The relationship of induced vertical force versus net vertical displacement for this same push-pull cycle is shown in Figure 10b. During both the compression and uplift cycles starting from zero induced force, the geopier foundation system stiffens with increasing displacement or force. This stiffening effect is more pronounced in compression than in uplift. Thus, the geopier system had a high factor of safety against failure at the peak forces or displacements for both compression and uplift.

## CONCLUSIONS

The geopier foundations supporting the structural reaction frame in these full-scale simulated seismic tests performed well. The foundations were subjected to large cyclic lateral and uplift-compression loads as well as significant overturning moments produced by the horizontal forces. For the conditions of the tests, including large loads, poor subsurface soils, and no embedment of the foundations, the magnitudes of the maximum displacements and rotations were relatively

small. Furthermore, the permanent displacements at the end of the tests were small. Overall, the results indicate that geopier foundations are ductile and can sustain large displacements—such as those generated by earthquakes—without significant damage and thereby can maintain serviceability after an earthquake.

Specific major results and conclusions determined from these tests are summarized as follows:

1. For one loading cycle analyzed, 95 percent of the vertical compressive load applied to the foundation system at the bearing level was carried by the geopiers. The footing contact stresses induced on the geopiers ranged from about 25 to 45 times the contact stresses induced on the matrix soil.
2. Equations developed previously (1) for estimating the induced contact stresses on the geopiers and matrix soil based on subgrade reaction theory were found to provide reasonable estimates of the measured stresses.
3. During uplift of the foundations, the measured induced compressive stresses within the instrumented geopier were greatest at the bottom and decreased with decreasing depth. These results confirm that uplift loads are transmitted to the ground through the uplift plates at the bottoms of the geopiers.
4. Even without being embedded, the geopier foundation system provided significant resistance to sliding from lateral loads. This resistance was derived primarily from shearing resistance along the geopier-footing interfaces and passive resistance from the uplift bars pushing on the geopier material. Numerical analyses indicate that the portion of lateral resistance provided by the uplift bars was between 21 and 42 percent of the peak lateral force generated during the test.
5. The permanent displacements at the end of the test were small.

## ACKNOWLEDGMENTS

The author is grateful to Wasatch Constructors for allowing these tests to be conducted. Without their permission and cooperation, this research could not have been undertaken.

Funding for this project was provided by the Utah Department of Transportation (UDOT) and FHWA, the National Science Foundation, Geopier Foundation Company Inc., and the University of Utah.



ConeTec performed the CPTs without charge. Dywidag Systems International USA provided the uplift bars at their cost.

Special thanks go to the author's colleagues at the University of Utah. Scott Merry was instrumental in providing expertise related to instrumentation and data acquisition. Chang-Lin Hsu was the primary student who assisted with the work. Chris Pantelides was responsible for the structural portion of the research.

Help from the UDOT Research Division was critical to the success of this research. In particular, Sam Musser and Steven Bartlett conducted oversight and management duties, acted as liaisons with personnel from Wasatch Constructors, and provided helpful suggestions.

Woodward-Clyde and Terracon provided significant information regarding the properties of the soils in the I-15 corridor.

Geopier Foundation Company Northwest provided engineering and supervisory personnel to the project at no cost. Particular thanks are due John Martin, Sr., John Martin, Jr., and James Johnson for donating their time.

Many other people also contributed to the project, and their assistance is gratefully acknowledged.

## REFERENCES

1. Lawton, E. C., and N. S. Fox. Settlement of Structures Supported on Marginal or Inadequate Soils Stiffened with Short Aggregate Piers. In *Vertical and Horizontal Deformations of Foundations and Embankments*. Geotechnical Special Publication 40, ASCE, New York, 1994, Vol. 2, pp. 962-974.
2. Lawton, E. C., N. S. Fox, and R. L. Handy. Control of Settlement and Uplift of Structures Using Short Aggregate Piers. In *In-Situ Deep Soil Improvement*. Geotechnical Special Publication 45 (K.M. Rollins, ed.), ASCE, New York, 1994, pp. 121-132.
3. Terzaghi, K. Evaluation of Coefficients of Subgrade Reaction. *Geotechnique*, Vol. 5, No. 4, Dec. 1955, pp. 297-326.
4. Lawton, E. C. *Performance of Geopier Foundations During Simulated Seismic Tests at South Temple Bridge on Interstate 15, Salt Lake City Utah*. Report No. UUCVEEN 99-06. Department of Civil and Environmental Engineering, University of Utah, Salt Lake City, June 1999.
5. Reese, L. C., L. A. Cooley, and N. Radhakrishnan. *Laterally Loaded Piles and Computer Program COM624G*. Technical Report K-84-2. U.S. Army Corps of Engineers Waterways Experiment Station, Vicksburg, Miss., 1984.

---

*Publication of this paper sponsored by Committee on Foundations of Bridges and Other Structures.*

TRANSPORTATION RESEARCH

# RECORD

**JOURNAL OF THE TRANSPORTATION RESEARCH BOARD**

---

NO.

1736

## **Soil Mechanics 2000**

Soils, Geology, and Foundations

A PEER-REVIEWED PUBLICATION OF THE TRANSPORTATION RESEARCH BOARD

---

TRANSPORTATION RESEARCH BOARD – NATIONAL RESEARCH COUNCIL

NATIONAL ACADEMY PRESS  
Washington, D.C. 2000